





Original Research

The α -Gal KO Mouse Animal Model is a Reliable and Predictive Tool for the Immune-Mediated Calcification Assessment of Heart Valve Bioprostheses

Filippo Naso^{1,*}, Alessandro Gandaglia¹, Giulio Sturaro¹, Cesare Galli²,
Robert J. Melder³

¹Biocompatibility Innovation Srl, IT-35042 Este, Padua, Italy

²Avantea, IT-26100 Cremona, Italy

³Mountain Hawk Consulting LLC, Glen Allen, VA 23059, USA

*Correspondence: f.naso@biocompatibility.bio (Filippo Naso)

Academic Editor: Natascia Tiso

Submitted: 19 January 2024 Revised: 26 March 2024 Accepted: 10 April 2024 Published: 10 May 2024

Abstract

Background: Recent studies highlighted the presence of anti- α -Gal antibodies in patients implanted with commercial bioprosthetic heart valves (BHVs). BHVs expose residual α -Gal xenoantigen and their recognition by the circulating anti-Gal antibodies leads to opsonization of the device's tissue component with the consequent triggering of a deterioration pathway that culminates with calcification. Small animal models such as mice and rats have been broadly involved in the *in vivo* testing of biomaterials by subcutaneous implantation, especially for the effectiveness of BHVs anti-calcific treatments. However, since models employed for this purpose express α -Gal antigen, the implantation of BHVs' leaflets does not elicit a proper immunological response, so the calcification propensity may be dramatically underestimated. **Methods:** An α -Gal knockout (KO) mouse model has been created, using the CRISP/Cas9 approach, and adopted to assess the calcification potential of commercial BHVs leaflets through the surgical implantation in the back subcutis area. Calcium quantification was performed by inductively coupled plasma analysis; immune response against the BHVs leaflets and α -Gal silencing was evaluated through immunological assays. **Results:** Two months after the implantation of commercial BHV leaflets, the anti-Gal antibody titers in KO mice doubled when compared with those found in wild-type (WT) ones. Leaflets explanted from KO mice, after one month, showed a four-time increased calcium deposition concerning the ones explanted from WT. The degree of silencing of α -Gal varied, depending on the specific organ that was assessed. In any case, the animal model was suitable for evaluating implanted tissue responses. **Conclusions:** Such mouse model proved to be an accurate tool for the study of the calcific propensity of commercial BHVs leaflets than those hitherto used. Given its reliability, it could also be successfully used to study even other diseases in which the possible involvement of α -Gal has been observed.

Keywords: α -Gal antigen; bioprosthetic heart valves; calcification; knockout mouse model; GGTA1^{-/-}; CRISP/Cas9; xenograft

1. Introduction

Cardiovascular diseases rank among the primary causes of mortality globally and addressing them appropriately continues to be a significant challenge in clinical practice. Among these, calcific aortic valve disease represents one of the most challenging issues worldwide with a high associated mortality rate that of 41% and 52% after 5 years, for mild and severe aortic stenosis respectively. Due to a lack of approved pharmaceutical treatments, the only usable clinical approach is the surgical replacement of the valve with prosthetic heart valves [1–3]. Among the various options, the most used involves the implantation of bioprosthetic heart valve (BHV) substitutes, usually made of pericardial tissue of bovine or porcine origin [4]. Such BHVs are fixed with glutaraldehyde (GA) for the improvement of the mechanical properties, assuring sterility and stability, as well as the reduction of immunogenicity. These devices are usually implanted in older people (>60 years) in whom the

expectation of the bioprosthetic function should be higher than the patients' lifetime; indeed, BHVs are infrequently used in younger patients because of their propensity to calcify, a process that is even more rapid in this type of patient because of their more active calcium metabolism and a more aggressive immune system [5]. Historically, calcification of BHVs has been ascribed to multiple external elements, as, for example, variability of GA bounds to the extracellular matrix (ECM), stress-related breakdown, and internal factors such as collagenolytic process and calcium deposition induced by remaining phospholipids [6]. Recently, the intrinsic pathway mediated by the immune system has become noteworthy, primarily due to recognition of the α -Gal xenoantigen trigger [7,8].

The α -Gal epitope (Gal α 1-3Gal β 1-4GlcNAc-R) represents a unique polysaccharide structure naturally produced on glycolipids, glycoproteins, and proteoglycans in the vast majority of mammals [9]. Although present in non-primate mammals, prosimians, and New World mon-



keys, it is not naturally expressed in Old World monkeys, apes, and humans that instead normally produce antibodies against it, due to the expression of the antigen on the bacterial wall of the resident gut flora [10,11]. The continued stimulation from these bacteria forces the immune system to produce anti-Gal antibodies that represent 1–8% and 1–2.5% of the circulating IgM and IgG human immunoglobulins, respectively [12,13].

The choice to use rats or mice for *in vivo* biomaterial assessment, is a common practice, due to their cost-effectiveness, ready availability, manageability, and clearly defined immunological patterns. These animals are frequently employed to study the chronic changes that affect contemporary or novel BHVs' leaflets when placed in a subcutaneous dorsal area. Specifically, the subdermal model guarantees a good serum and blood exposition of the implant ensuring cellular migration and enabling a reliable evaluation of anti-calcification treatments [14,15].

Nevertheless, implanting BHV leaflets (mainly sourced from bovine or porcine pericardium) into a wild-type (WT) mouse represents a concordant xenotransplantation scenario with respect to the α -Gal xenoantigen. In this scenario, both donor and recipient species exhibit this epitope, thereby excluding the opportunity to examine the role of an immune response against α -Gal or the presence of preformed anti- α -Gal antibody and thus negating evaluation of the effects thereof instead, recognition occurs *in situ* within the α -Gal negative patient.

This study described the creation of a knockout (KO) mouse, genetically modified to be α -Gal deficient by suppressing the gene responsible for α 1,3-galactosyltransferase (GGTA1). This animal model should replicate more predictably the behavior of the human's immune system and the response to the presence of the xenoantigen by acquiring the ability to produce anti-Gal antibodies [16].

The primary target of the experimentation was to estimate calcium deposition in isolated leaflets from a surgical commercial BHVs of bovine pericardial origin implanted for 1, 2, and 4 months in GGTA1 KO mice, comparing it with an investigation conducted simultaneously in WT mice. Moreover, the possible remnant α -Gal epitopes in various tissues and organs of the KO mice were also evaluated, taking into consideration prior observations of residual reactivity in biallelic GGTA1-KO pig cells as a potential contributor to chronic rejection of GGTA1^{-/-} organs [17,18].

2. Materials and Methods

All surgical and experimental procedures conducted on animals followed the guidelines outlined in the Guide for the Care and Use of Laboratory Animals, as issued by the US National Institutes of Health (NIH Publication 85-23, revised 1996). The utilization of a mouse animal model for experimental purposes received approval from the Ital-

ian Ministry of Health under project registration number 17E9C.154 and authorization number 542/2020-PR. The GGTA1 KO mouse animal model is the property of BCI - Biocompatibility Innovation Srl (Este, Padua, Italy). The model generation process was conducted in cooperation with PolyGene Transgenetic (Rümlang, Switzerland), and the animals are presently homed at Charles River Laboratories Italia (Lecco, Italy).

2.1 Generation of C57Bl/6 α -Gal KO Mice

To knockout the *GGTA1* gene, the CRISP PolyGene I139 (PolyGene, Rümlang, Zürich) construct was used. The target exon of the intended gene was Ggta1-202_3. gRNAs for *GGTA1* were designed using the publicly available algorithm from the Institut des Neurosciences [19]. The algorithm returned several possible guides, but only the two with the best specificity were chosen and used.

2.1.1 Embryonic Stem (ES) Cells Targeting

ES cell lines used in the generation of chimeras were validated by STR profiling and tested negative for mycoplasma. 12000 ES cells were plated onto 6 cm plates and lipofected with 1 μ g of both guide plasmid and the homology oligo in each region (Lipofectamin LTX, Invitrogen, Waltham, MA, USA). Following a 24-hour incubation period, the cells underwent a 48-hour selection phase with 0.8 μ g/mL puromycin. This selection aimed to isolate cells expressing the guide/Cas9 plasmids temporarily. Subsequently, after an 8-day interval, 48 clones were chosen from each guide. These selected clones, exhibiting visibly reduced amplicon sizes during Polymerase Chain Reaction (PCR) screening, were then expanded into a 24-well plate and cryopreserved at -80°C . Further validation included retesting through PCR and sequencing. Despite a low yield of clones displaying visible deletions, six potential candidate clones were successfully identified. PCR was performed on the obtained clones using these primers:

I139.5 5'-GGATGCTGGGAAGTGAATCG-3'

I139.6 5'-AGGAGCACGGCATGAAAG-3'

The screening PCR utilizing primers I139.5/6 produces a 436 bp wild-type amplicon, a size conducive to detecting small deletions while still allowing for the identification of deletions within the range of 2–300 bp. Upon sequencing the candidate clones, the following results were obtained:

- Clone 3C8: 34 bp deletion and Loss of Heterozygosity (LOH)
- Clone 3C12: wild type
- Clone 3D7: 71 bp deletion and wild type
- Clone 4E3: 110 bp deletion and LOH
- Clone 4E7: 75 bp deletion/2 bp deletion
- Clone 4E8: 32 bp deletion and LOH

It is noteworthy that LOH, resembling homozygosity, is often misconstrued as such in CRISPR generation. In the mentioned cases, it is evident that distinct vari-

ants/mutations are highly improbable to occur simultaneously on corresponding alleles, suggesting a preferential amplification of the mutant and thus seemingly mutant-specific sequence information. Notably, it appears that the wild-type band, or at least a band of similar size to the wild type, is present in 3C8, 4E3, and 4E8, even if with a weaker intensity.

2.1.2 Germ Line Breeding and Genotyping

Nominee clones were inoculated into C57Bl/6Ng blastocysts with high effectiveness. The procedure allows 80–100% chimeric males to be obtained from each litter born in three of the clones used. To evaluate germ line transmission 11 of the chimera mice resulting from blastocyst inoculations were paired with C57Bl/6Ng mice. Since 3C8 mice did not breed satisfactorily, it was decided not to pursue this further and focus on more successful breeding clones. Additionally, the deletion size in 3C8 appeared less appealing. Interestingly, mice from 3D7 exhibited segregation into two sublines, one with a characterized 71 bp deletion and another with an 18 bp deletion. All pups displayed either of the deletions, indicating a clean heterozygous configuration. The 18 bp deletion, located within exon 4 but 55 bp downstream of the start of the 71 bp deletion, was not visible in the overlap PCR. Despite its small size, the 18 bp deletion was challenging to identify on the agarose gel. Consequently, it was initially mistaken for the 2 bp deletion in clone 4E8, leading to breeding; however, all corresponding mice were later eliminated. Subsequent inspection clarified that 4E8 had not produced chimeric offspring. Screening for deletions utilized primers I139.5 and I139.6. Clone 3D7 (bearing 71 bp deletion) and clone 4E7 (bearing 75 bp deletion) were bred with high productivity and showed a Mendelian distribution in D71 (20/42 mice; all others D18) and D75 (23/40). Numerous pairs of D71 and D75 mice were established for breeding to generate homozygous F2 mice. A total of 227 F2 mice were generated, with 152 from the D71 and D75 breedings. The ratios in these mice were fairly accurate Mendelian ratios, suggesting no discernible effect on development or viability for the mutant heterozygous or homozygous genotypes. To reaffirm the genotypes, several homozygous mice were sequenced using the I139.5/6 PCR and I139.5 as a Sanger sequencing primer, corroborating the sequencing data obtained in ES cells.

2.2 Quantification of α -Gal in WT and KO Mice Tissues

Around 100 mg wet weight of fresh tissue samples from different organs of both WT and KO mice were collected. Samples were then incubated with [1:50] M86 primary anti- α -Gal antibody (mouse; LSBio, Seattle, WA, USA) for 2 hs at 37 °C with mild agitation and spun at 15,000 rpm for 30 min at 4 °C. The quantification of α -Gal epitopes was conducted using a trademarked enzyme-linked immunosorbent assay (ELISA) test [20].

100 μ L of α -Gal/HSA (Human Serum Albumin) [5 mg/mL] per well (Dextra Laboratories, Berkshire, UK) were used for coating a 96-well Polysorp plate (Nunc, Rochester, NY, USA) for 2 hs at 37 °C. The plate was then washed thrice with DPBS (Dulbecco's Phosphate Buffered Saline) and nonspecific binding sites were saturated by incubation with 300 μ L per well of HSA (Sigma, St. Louis, MO, USA), 2%w/v in DPBS, for 2 hs at room temperature. Following three additional washes, the plate was loaded with 100 μ L per well of supernatant obtained from both WT and KO mice samples and incubated overnight at 4 °C. After incubation the plate was washed again and the M86 antibody was recognized by adding 100 μ L per well of secondary HRP-conjugate antibody [1:500] (Dako Cytomation, Glostrup, Denmark).

The signal was obtained by adding 100 μ L per well of horseradish peroxidase substrate buffer incubated for 5 min and by reading the absorbance at 450 nm with Multiscan Sky plate reader (Thermo Scientific, Waltham, MA, USA). Epitope number calculation was generated with a calibration line obtained using rabbit red blood cells [21].

2.3 Mouse Subcutaneous Implantation

GGTA1^{-/-} (C57BL/6, 6 weeks old) and WT (n = 16) mice were anesthetized and shaved; a subcutaneous pocket was created for each mouse in the dorsal area. A portion size of 1 cm \times 1 cm was isolated from leaflets of commercial GA-fixed BHV of bovine origine, and implanted singularly in the pocket of each animal, and the wounds were closed with 6/0 nylon sutures. After 1, 2, and 4 months, the mice were euthanized in a CO₂ atmosphere and samples were carefully collected (Fig. 1). As control to evaluate the potential contribution of the surgical insult to the immunological stimulation n = 3 KO mice (surgical insult cohort) underwent the same procedure without the implant of the leaflet.

2.4 Quantification of Anti-Gal Antibodies in GGTA^{-/-} Mouse

IgM and IgG anti-Gal antibodies in the serum of KO mice were assessed both before and 2 months after BHV's leaflet implantation using an ELISA test. Approximately 0.75 mL of blood per mouse was collected through infraorbital venous plexus sampling (n = 10). A Polysorp 96-well plate (Nunc) was coated with 100 μ L of α -Gal/HSA [5 mg/mL], for 2 hs at 37 °C. The plate was washed thrice with DPBS and saturation of nonspecific binding sites was conducted using 300 μ L per well of HSA 2%w/v in DPBS for 2 hs at room temperature. Following three washes, a set of wells was loaded with 100 μ L of [1:80] diluted serum and incubated overnight at 4 °C. After incubation the plate was washed again and secondary HRP-conjugate anti-mouse IgM and IgG antibodies [1:500] (Jackson ImmunoResearch, West Grove, PA, USA) were applied. Finally, the signal was obtained by adding 100 μ L per well of

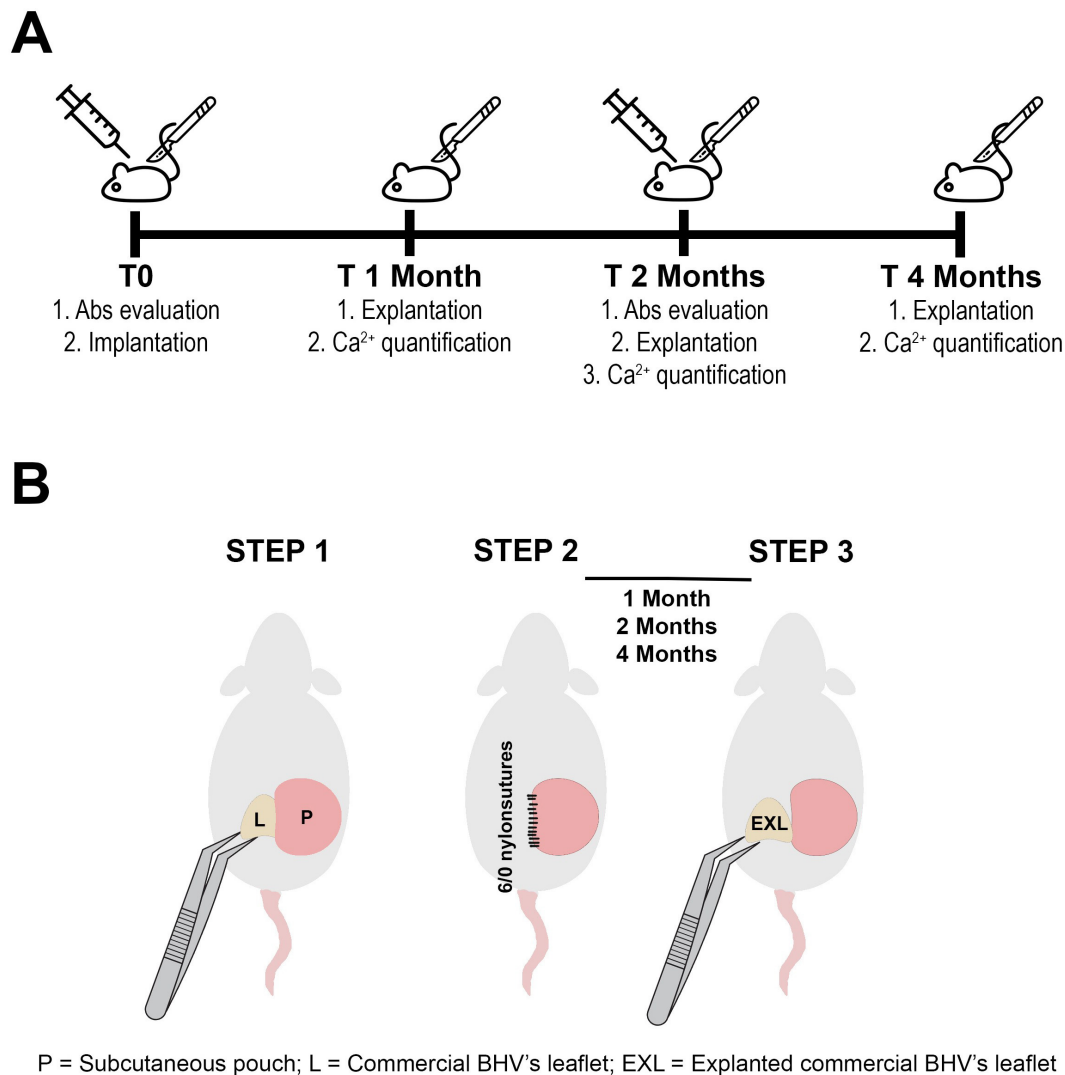


Fig. 1. Experiment timeline and schematic implant procedure. (A) Study timeline (Abs = antibodies). (B) Schematic representation of subcutaneous surgical implant of commercial BHV's leaflet. BHV leaflets (L) were inserted in a subcutaneous pouch (P) in the dorsal area of the animal (STEP 1). Pouch was sutured with 6/0 nylon (STEP 2). Explanted commercial BHV leaflets (EXL) were carefully harvested after 1, 2, and 4 months of incubation (STEP 3). BHVs, bioprosthetic heart valves.

horseradish peroxidase substrate buffer incubated for 5 min and by reading the absorbance at 450 nm with Multiscan Sky plate reader (Thermo Scientific).

2.5 Calcium Quantification

Leaflets of the tested BHV were carefully removed from both KO and WT animals and washed twice in sterile cold PBS for 10 min. Subsequently, the samples underwent acid hydrolysis in HCl 6N at 110 °C for 12 hs. Calcium assessment in hydrolyzed samples was conducted using inductively coupled plasma spectroscopy following EPA 6010D method's guidelines [22] and reported as $\mu\text{g Ca}^{2+}/10 \text{ mg}$ of dry defatted weight (ddw).

The same evaluation carried out on un-implanted, off-the-shelf, valve leaflets was taken as a control. The determination of ddw was made by comparing lyophilized

dry-weight samples before and after delipidation treatment. Following the lyophilization step, tissue samples were incubated for 36 hs under 10 kPa over P_2O_5 at 37 °C until a constant dry weight was achieved. The defatting method was carried out by first incubating the tissue samples in an ascending series of alcohols, followed by two phases of chloroform/methanol (2:1 and 3:1 v/v), and then in a descending series of alcohols and finally in water.

2.6 Statistical Analysis

Data were analyzed in Microsoft Excel® and Prism®7 for Windows (v7.03, GraphPad Software Inc., San Diego, CA, USA) and expressed as mean \pm standard deviation (SD). A one-sided unpaired *T*-test was used to assess significant differences between the two groups, at the 0.95 confidence level.

Table 1. Expression of α -Gal epitopes per 10 mg in different tissue districts of WT e GGTA1 KO mice with the relative percentage of silencing (n = 7 for each tissue district).

α -Gal distribution in KO and WT mice			
Tissue/Organ	% of α -Gal silencing	KO	WT
Eye	100%	0	$7.68 \times 10^{11} \pm 0.08$
Spleen	100%	0	$1.70 \times 10^{11} \pm 0.02$
Tail	100%	0	$4.13 \times 10^{11} \pm 0.05$
Thymus	100%	0	$5.26 \times 10^{11} \pm 0.05$
Myocardium	86.3%	$2.08 \times 10^{10} \pm 0.01$	$1.52 \times 10^{11} \pm 0.02$
Kidney	82%	$2.76 \times 10^{10} \pm 0.02$	$1.53 \times 10^{11} \pm 0.03$
Lung	80%	$5.86 \times 10^{10} \pm 0.02$	$2.93 \times 10^{11} \pm 0.03$
Liver	80%	$4.10 \times 10^{10} \pm 0.03$	$2.05 \times 10^{11} \pm 0.06$
Skin	44.4%	$9.55 \times 10^{10} \pm 0.05$	$1.72 \times 10^{11} \pm 0.01$
Brain	44.2%	$1.87 \times 10^{10} \pm 0.02$	$3.35 \times 10^{11} \pm 0.02$

WT, wild-type; GGTA1, α 1,3-galactosyltransferase; KO, knockout.

3. Results

3.1 Quantification of α -Gal in WT and GGTA^{-/-} Tissues

Table 1 shows that *GGTA1* gene silencing determined the inhibition of α -Gal antigen synthesis unevenly, varying from 100% to 80%, based on tissue compartment. Notably, for both skin and brain specimens, inhibition of antigen expression was restricted to 44%. An intriguing observation is that the brains of the WT mice display the fewest number of α -Gal antigens, despite representing the similar number of epitopes determined in KO mice following gene silencing.

3.2 Evaluation of anti-Gal Antibodies Production in GGTA^{-/-} Mice

Due to food uptake during growth, KO mice develop a microbial flora expressing α -Gal antigen, resulting in the instauration of a baseline level of IgG and IgM anti- α -Gal antibodies. This baseline level seems to be raised further upon implantation of BHV leaflets, which are known to contain a considerable amount of this antigen [23]. In this particular case, the two months of implantation in the mouse subcutis doubled the level of circulating anti-Gal IgG and more than tripled that of IgM (Fig. 2). The analysis of the surgical insult cohort reported no statistically significant differences in IgG and IgM antibody levels compared to the baseline (data not shown).

3.3 Calcium Quantification in Explanted Leaflets

As reported by Fig. 3, the leaflets of the commercial BHV explanted from KO mice, show a significant calcium deposition (green bar) after just one month, surpassing more than fourfold the quantity detected in the WT mouse (yellow bar) during the equivalent period (1 month KO vs. 1 month WT, $p = 0.005$). Despite an escalation in mineralization intensity after 2 and 4 months, significant differences were not observed between the KO and WT mice ($p < 0.05$).

4. Discussion

BHV degeneration appears as a multimodal process engaging mechanical, chemical, and immunological pathways, leading to structural degradation over different time frames [24]. To date, GA still represents the gold standard fixative and sterilizing agent for almost all BHVs available on the market. Unfortunately, GA possesses an intrinsic chemical instability that consequently leads to a host immune response which is the first step in an articulated series of mechanisms that result in tissue calcification. The deposition of calcium is mainly due to the presence of the free aldehydic and carboxylic groups, which can attract Ca^{2+} ions becoming then stuck in the fibers of the tissues. The Ca^{2+} ions deposited act then as a nucleation site for other ions that are attracted by Van der Waals forces slowly generating crystals. This process is exacerbated also by the fact that GA treatment induces chemical changes in proteins within the tissue, altering their structure and composition, and making the tissue even more susceptible to interactions with calcium. Such denaturation may expose previously hidden sites that are prone to calcium binding [25].

To mitigate the impact on the calcification process, BHV manufacturers have proposed various modifications to GA fixation protocols. These modifications include additional steps aimed at chemically stabilizing reactive chemical groups. Processes such as GA detoxification by urazole, diamine spacer extension, treatment with 2-amino oleic acid, or incubation in ethanol are among the strategies developed to enhance GA stabilization, to delay calcific tissue dystrophy [26,27]. Besides BHV calcification, which usually occurs over a long period (average of 10 years in >60 years people), several degenerative processes have also been found to occur within a very short time frame, even hours, immediately following implantation. These rapid mechanisms are attributable to the action of the patient's immune system towards the implant [28]. The Translink international collaborative study group has recently highlighted this aspect. The study confirms that

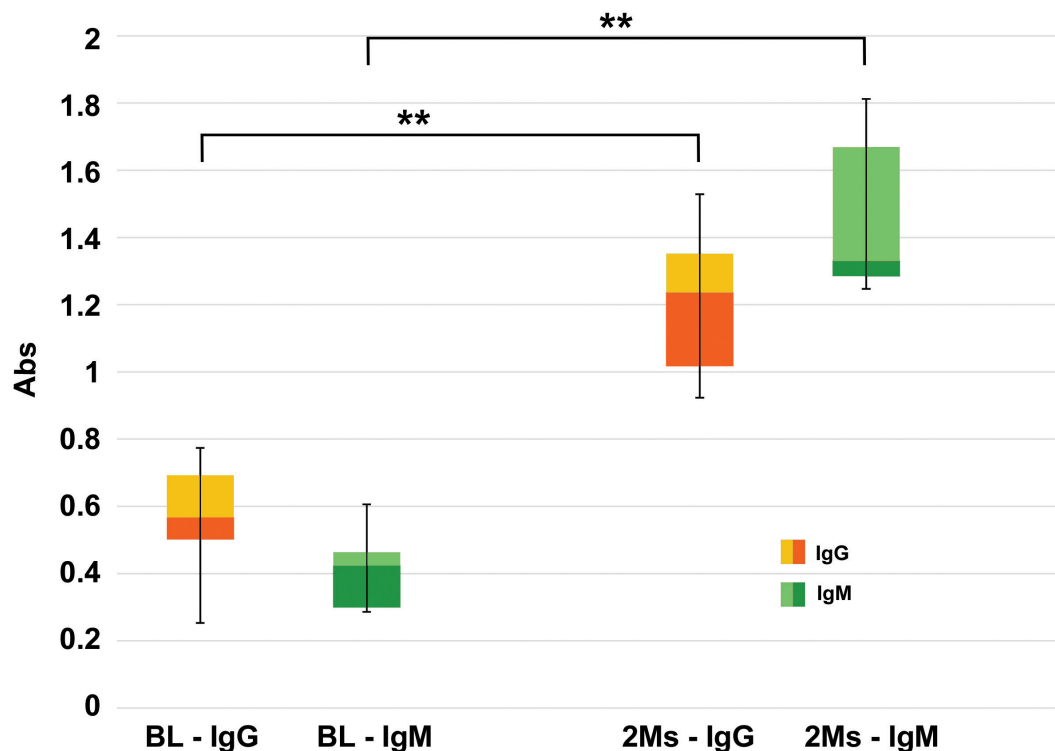


Fig. 2. Evaluation of anti-Gal antibodies. Quantitative evaluations of anti-Gal IgG and IgM antibodies production in KO mice after 2 months (2 Ms) of commercial BHVs leaflets subcutis implant compared to the basal level (BL), evaluated before the tissue implant. Data are expressed as absorbance units (450 nm), $n = 10$ for each type of sample. Data points represent the means \pm standard deviation (SD). ** indicates a statistically significant difference ($p < 0.05$).

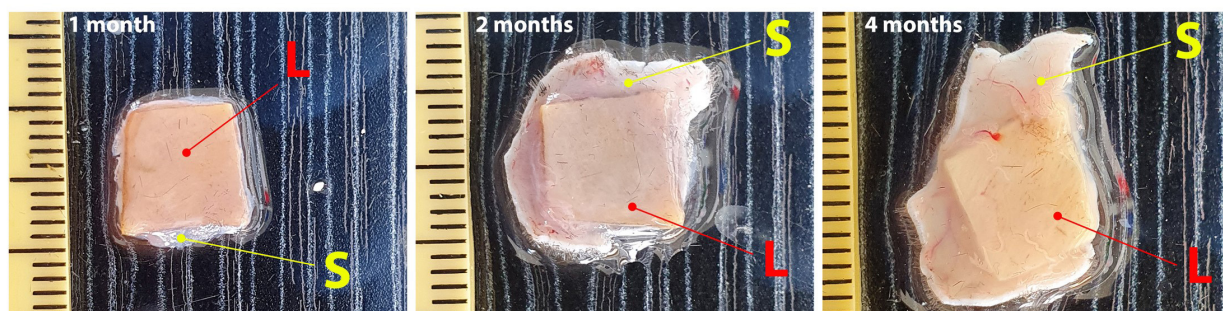
preformed antibodies generate an immune response that exacerbates calcification processes due to remaining antigens on BHV tissue [7,8]. The obtained results are in line with what was already observed in the Translink study. The absence of α -Gal in the KO model was paired with a rapid (one-month) immune response that led to a deposition of calcium that was four times higher than the one observed in WT animals in the same time. This rapid and severe response mimics what is, unfortunately, widely observed in young patients that undergone valve replacement in which the prosthesis fails due to calcification in a very short period [29,30]. As already reported, the remnants α -Gal xenoantigens starts to increase the anti-Gal antibody titers about two weeks after the implantation of the bioprosthetic device. The antibody titers continue to rise over time reaching a peak in 3–4 months specially for IgG and IgM isotype. Once raised, the levels of these antibodies do not return to basal levels even after 5 years from implantation. This fact may be easily ascribed to the instability of the crosslink with GA. Such chemical instability, emphasized by the mechanical stress to which BHVs are subjected, is involved in the breaking down of the GA network, exposing previously masked xenoantigenic epitopes. In this way, a mild but continuous immunological stimulation is maintained with the subsequent antibody formation [31,32]. After the BHV leaflet implant, the GGTA1 KO animal model

exhibited an increase in the IgG and IgM anti-Gal antibody titers similar to what was already observed in humans [33].

Thanks to their low cost, ready availability, ease of handling, and well-defined immune parameters, small animal models such as rats and mice are a common and practical choice for *in vivo* study of biomaterials. However, in the majority of the cases, the selected models are WT, preventing the possible immunological implications in the studied process. Conversely, the use of an α -Gal KO model permits also to evaluate the implication of the immunomediated mechanisms alongside intrinsic and extrinsic ones that are already assessed by using WT models. Noteworthy, the findings from this study serve to reaffirm the existence of immunologically active α -Gal antigen in BHVs currently utilized in clinical practice, as determined previously through an alternative analytical method [23].

The GGTA1 gene, silenced in the model under investigation in this study, encodes for α 1,3 GT galactosyltransferase enzyme that catalyzes the formation of the α -Gal epitopes. This reaction involves the formation of an α -(1,3)-glycosidic bond between a galactose and an N-acetyllactosamine (LacNAc) (Fig. 4) acceptor molecule present on both protein and lipid on cells' plasma membrane [34]. However, this is not the only enzyme to catalyze this reaction. Milland and colleagues [35] have described the presence of isoglobotrihexosylceramide synthase (iGb3s)

A



B

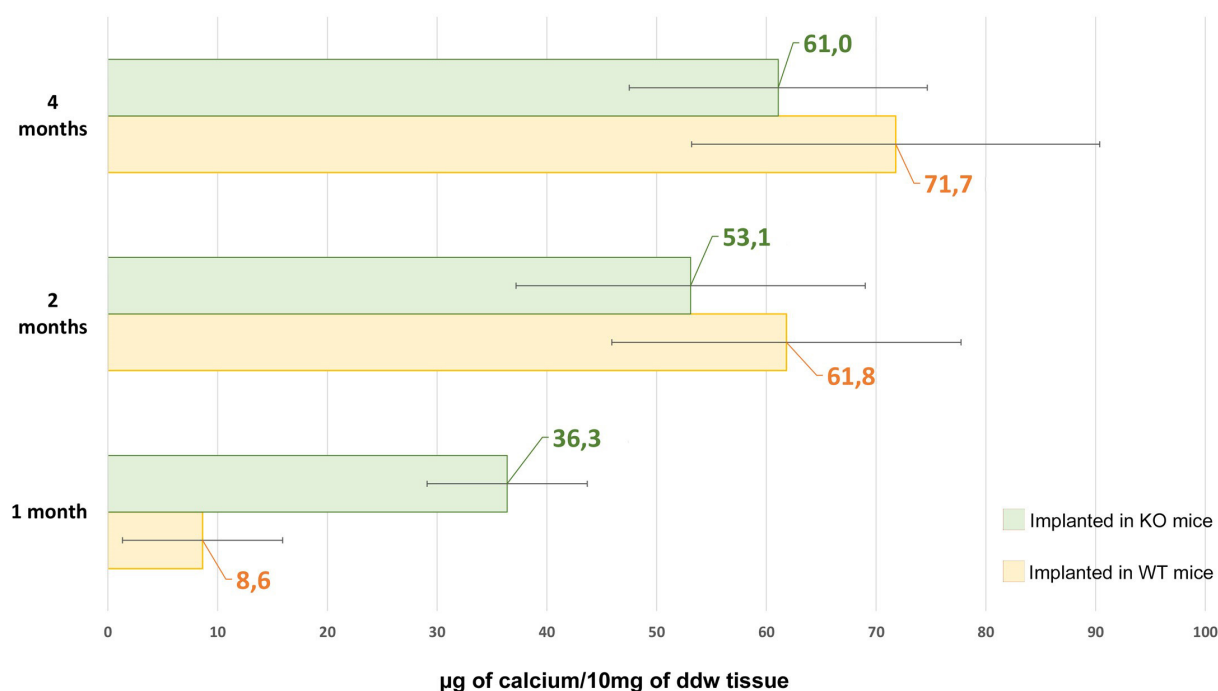


Fig. 3. Calcium evaluation in explanted leaflets. (A) Representative photos of explanted leaflet tissue after 1, 2 and 4 months of implantation (L = leaflets; S = skin). (B) Quantitative evaluation of calcium deposits in commercial BHVs leaflet implanted in the back subcutis area of Knockout (KO) (green bars) and Wild-type (WT) (yellow bars) mice at 1, 2, and 4 months. As a control sample, calcium quantification was also carried out in non-implanted off-the-shelf commercial BHV leaflets resulting in $1.19 \pm 0.05 \mu\text{g}/10 \text{ mg}$ of ddw. 1 month WT vs. KO $p < 0.05$; 2, and 4 months WT vs. KO $p > 0.05$.

in GGTA1 KO mice that bond galactose exclusively to glycosphingolipids (Lac). This is the reason why a residual presence of α -Gal epitopes has been still detected in biallelic GGTA1 KO pig animal model and this could be implicated in the rejection of GGTA1^{-/-} organs found exploring xenotransplantation in non-primate models. This study reported a residual presence of α -Gal in the KO model, varying concerning the analyzed tissue district (Table 1), which is in line with what can be found in the literature.

From the collected data, α -Gal results not completely silenced in the brain, and skin, which are tissues that featured a high presence of ceramides. As mentioned above, the iGb3s enzyme generates α -Gal epitope exclusively capping lipids, mainly ceramides. For this reason, it is possi-

ble to observe residual α -Gal epitope where an alternative pathway may restore function. In addition, the conduction of nerve impulses in mammals, both centrally and peripherally, is enabled by the presence of the myelin sheath that surrounds axons. The myelin sheath is a lipid-rich membrane of which 30% is composed of galactosylceramides (GalCer). Interestingly, GalCers' levels are particularly high in the brain where they were seen to be also higher than the ones observed in WT models [36]. Several studies have highlighted the importance of ceramides in the brain: they mediate signal transduction and cell adhesion and are critical for the development of nervous tissues; this should explain why significant numbers of iGb3s- α -Gal epitopes are also present in KO mice, the presence of which is unavoid-

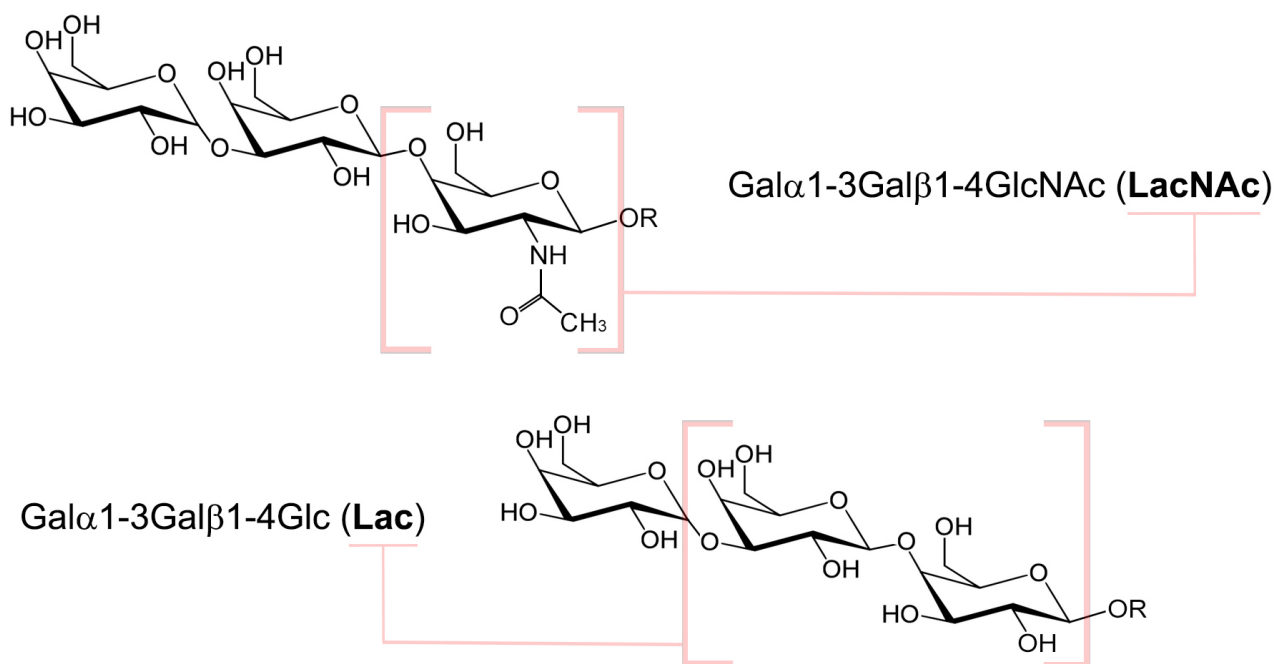


Fig. 4. Chemical structure of the two different types of the α Gal epitopes synthesized by GGTA1 (NAc) or iGb3 (Lac) enzyme. The presence of NAc or Lac determines the immunogenicity of the whole structure.

able for proper brain and neuronal function [37]. Prominent expression of ceramides is also present in the stratum corneum of the epidermis of the mammals, which represents the outermost layer. It is composed of flattened, enucleated keratinocytes and a unique extracellular lipid matrix produced by differentiating keratinocytes and it presents a permeability barrier towards water, chemicals, and microorganisms [38]. A significant presence of ceramides is also found in the myocardium, liver, lungs, and kidneys [39]. The residual presence of α -Gal detected in this study is in line with the study of Shao and colleagues who describe a reduction in the expression of the antigen between 5.19% and 21.74% in GGTA1-KO mice, apart from the skin and brain where, due to a higher concentration of ceramides, the reduction is much smaller [40].

It is important to underline that the presence of iGb3s in the KO model is not sufficient to trigger an immune response that involves the destruction of the cells presenting the epitope. This fact was validated by the work of Murray and colleagues who found that it is necessary to have a minimum basal level of α -Gal for antibody-mediated rejection to occur in a GGTA1 KO mouse model [41].

In 2016 Butler and colleagues [42] demonstrated that the silencing of the porcine iGb3S gene did not impact assessments of expected acute rejection in pig-to-human and pig-to-primate xenotransplantation showing that iGb3S does not play a role in antibody-mediated rejection. The α -Gal contribution due to the presence of iGb3S is not appreciable by heat-inactivated human and baboon sera antibodies when incubated with GGTA1 KO or GGTA1/iGb3S double KO pig tissue [42]. This is the reason, even if

residues of α -Gal antigen are still present, the GGTA1 KO mouse was revealed as an adequate animal model for evaluating the calcification propensity of currently adopted BHV tissues.

Since other pathological conditions have been linked to variations in circulating anti-Gal antibodies in humans, this animal model could also prove useful for the development of novel diagnostic approaches. Our research group has recently demonstrated a variation in the levels of circulating anti-Gal antibodies in Alzheimer's disease patients compared with healthy subjects [43]. Since Alzheimer's disease is a condition in which the mechanisms are not yet fully established and the treatments not optimized, the possibility of being able to study it in a reliable animal model seems promising and could open new diagnostic rather than curative approaches. In addition, Dahl and colleagues [44] have seen that GGTA1 KO mouse models show glucose intolerance and reduced pancreatic β -cell function, opening up the possibility of studying diabetic diseases with this model. The same model also showed rapid development of cataracts, 3–6 weeks after birth, probably because of glucose intolerance, thus mimicking what occurs in humans [45,46]. This KO model is also useful in the study of wound healing, as it has been shown that the application of α -Gal-containing nanoparticles *in situ* increases endothelial migration and accelerates wound closure times [47]. Finally, such a model could help to better understand the mechanisms underlying the onset of the α -Gal syndrome. This syndrome, which most often initiates when a Lone Star tick bites a subject, is an allergic reaction that sometimes manifests in severe forms that can be life-threatening. It is trig-

gered when the patient encounters α -Gal-containing products, such as red meat, milk, and even some drugs. This syndrome has been growing in importance in the United States in recent times due to an increasing number of diagnosed cases so much so that FDA approved the use of α -Gal KO pigs for human food and potential therapeutic uses [48,49].

Given the increasing attention being focused on α -Gal and its repercussions on human health, the possibility of being able to use large KO animals such as cattle and pigs for medical as well as food purposes opens up new perspectives for treatment, especially in the cardiovascular field. Indeed, animals, genetically engineered to not express α -Gal and other xenoantigens such as Neu5Gc [50,51], could be a promising source of organs and tissues, as recently demonstrated by the first two KO pig heart transplants in human patients which successfully avoided the hyperacute rejection reactions [52,53].

5. Study Limitations

Small animal models, such as mice and rats have been widely used for years as a reliable tool for *in vivo* assessment of calcification propensity of biomaterials through subcutis implantation. This approach is technically easier and cheaper than implanting entire bioprostheses in large animals moreover, mice present an accelerated calcium metabolism that can mimic what is observed in clinical specimens especially in young patients [54]. However, the implanted biomaterial is not subjected to continuous blood flow and pressure or to any other mechanical stress to which a BHV may be subjected that can influence the calcification response.

6. Conclusions

The implantation of commercial BHV leaflets has been shown to activate the α Gal KO murine immune system, leading to a substantial generation of anti-Gal antibodies of both IgM and IgG classes. This immune response in mice appears to closely resemble the reactions observed in humans, as extensively documented in the literature. These findings underscore crucial factors in assessing the effectiveness of anti-calcific treatments, emphasizing the importance of selecting small animal models, favoring the KO model. This choice may be mandatory to prevent the potential risk of dramatically underestimating the impact of the immune-mediated reactions to xenoantigens.

Availability of Data and Materials

The authors declare that all datasets on which the conclusions of the manuscript depend are included in the study and are available to the readers.

Author Contributions

FN and AG designed the research study. GS and FN performed the research. RM and CG analyzed the data. GS

and FN wrote the manuscript. All authors have participated sufficiently in the work to take public responsibility for appropriate portions of the content and agreed to be accountable for all aspects of the work in ensuring that questions related to its accuracy or integrity. All authors contributed to editorial changes in the manuscript. All authors read and approved the final manuscript.

Ethics Approval and Consent to Participate

All animal experiments and surgical procedures adhered to the guidelines outlined in the Guide for the Care and Use of Laboratory Animals, as published by the US National Institutes of Health (NIH Publication 85-23, revised 1996). The utilization of a mouse animal model for experimental purposes received approval from the Italian Ministry of Health under project registration number 17E9C.154 and authorization number 542/2020-PR.

Acknowledgment

The GGTA1 KO mouse animal model was kindly supplied by Biocompatibility Innovation Srl.

Funding

This research received no external funding.

Conflict of Interest

Alessandro Gandaglia, Giulio Sturaro, and Filippo Naso are employees of Biocompatibility Innovation Srl. Robert J. Melder is a scientific consultant for Biocompatibility Innovation Srl. Cesare Galli declares no conflict of interest.

References

- [1] Zebhi B, Lazkani M, Bark D, Jr. Calcific Aortic Stenosis-A Review on Acquired Mechanisms of the Disease and Treatments. *Frontiers in Cardiovascular Medicine*. 2021; 8: 734175.
- [2] Stewart S, Afoakwah C, Chan YK, Strom JB, Playford D, Strange GA. Counting the cost of premature mortality with progressively worse aortic stenosis in Australia: a clinical cohort study. *The Lancet. Healthy Longevity*. 2022; 3: e599–e606.
- [3] Kraler S, Blaser MC, Aikawa E, Camici GG, Lüscher TF. Calcific aortic valve disease: from molecular and cellular mechanisms to medical therapy. *European Heart Journal*. 2022; 43: 683–697.
- [4] Ryu R, Tran R. DOACs in Mechanical and Bioprosthetic Heart Valves: A Narrative Review of Emerging Data and Future Directions. *Clinical and Applied Thrombosis/hemostasis: Official Journal of the International Academy of Clinical and Applied Thrombosis/Hemostasis*. 2022; 28: 10760296221103578.
- [5] Percy ED, Harloff M, Hirji S, Malarczyk A, Cherkasky O, Yazdchi F, *et al.* Subclinical Structural Valve Degeneration in Young Patients with Bioprosthetic Aortic Valves. *The Annals of Thoracic Surgery*. 2021; 111: 1486–1493.
- [6] Marro M, Kossar AP, Xue Y, Frasca A, Levy RJ, Ferrari G. Non-calcific Mechanisms of Bioprosthetic Structural Valve Degeneration. *Journal of the American Heart Association*. 2021; 10: e018921.
- [7] Senage T, Paul A, Le Tourneau T, Fellah-Hebia I, Vadori M,

- Bashir S, *et al.* The role of antibody responses against glycans in bioprosthetic heart valve calcification and deterioration. *Nature Medicine*. 2022; 28: 283–294.
- [8] Lila N, McGregor CGA, Carpentier S, Rancic J, Byrne GW, Carpentier A. Gal knockout pig pericardium: new source of material for heart valve bioprostheses. *The Journal of Heart and Lung Transplantation: the Official Publication of the International Society for Heart Transplantation*. 2010; 29: 538–543.
- [9] Macher BA, Galili U. The Gal α 1,3Gal β 1,4GlcNAc-R (alpha-Gal) epitope: a carbohydrate of unique evolution and clinical relevance. *Biochimica et Biophysica Acta*. 2008; 1780: 75–88.
- [10] Yehuda S, Padler-Karavani V. Glycosylated Biotherapeutics: Immunological Effects of N-Glycolylneuraminic Acid. *Frontiers in Immunology*. 2020; 11: 21.
- [11] Thall AD, Malý P, Lowe JB. Oocyte Gal α 1,3Gal epitopes implicated in sperm adhesion to the zona pellucida glycoprotein ZP3 are not required for fertilization in the mouse. *The Journal of Biological Chemistry*. 1995; 270: 21437–21440.
- [12] Galili U. The alpha-gal epitope and the anti-Gal antibody in xenotransplantation and in cancer immunotherapy. *Immunology and Cell Biology*. 2005; 83: 674–686.
- [13] Jaurigue JA, Seeberger PH. Parasite Carbohydrate Vaccines. *Frontiers in Cellular and Infection Microbiology*. 2017; 7: 248.
- [14] Christ T, Dohmen PM, Holinski S, Schönauf M, Heinze G, Konertz W. Suitability of the rat subdermal model for tissue engineering of heart valves. *Medical Science Monitor Basic Research*. 2014; 20: 194–199.
- [15] Ground M, Waqanivalagi S, Walker R, Milsom P, Cornish J. Models of immunogenicity in preclinical assessment of tissue engineered heart valves. *Acta Biomaterialia*. 2021; 133: 102–113.
- [16] Lee C, Ahn H, Kim SH, Choi SY, Kim YJ. Immune response to bovine pericardium implanted into α 1,3-galactosyltransferase knockout mice: feasibility as an animal model for testing efficacy of anticalcification treatments of xenografts. *European Journal of Cardio-thoracic Surgery: Official Journal of the European Association for Cardio-thoracic Surgery*. 2012; 42: 164–172.
- [17] Gasek N, Dearborn J, Enes SR, Pouliot R, Louie J, Phillips Z, *et al.* Comparative immunogenicity of decellularized wild type and alpha 1,3 galactosyltransferase knockout pig lungs. *Biomaterials*. 2021; 276: 121029.
- [18] Kuwaki K, Tseng YL, Dor FJMF, Shimizu A, Houser SL, Sanderson TM, *et al.* Heart transplantation in baboons using alpha1,3-galactosyltransferase gene-knockout pigs as donors: initial experience. *Nature Medicine*. 2005; 11: 29–31.
- [19] Tefor infrastructure. Version 5.01. 2022. Available at: <http://crispor.tefor.net> (Accessed: 17 January 2022).
- [20] Naso F, Gandaglia A, Spina M, Gerosa G, inventors. Method for detecting a xenoantigen infixed tissues used as bioprosthetic replacements. UE: European patent EP2626701. 8 February 2013.
- [21] Galili U, Rachmilewitz EA, Peleg A, Flechner I. A unique natural human IgG antibody with anti-alpha-galactosyl specificity. *The Journal of Experimental Medicine*. 1984; 160: 1519–1531.
- [22] U.S. Environmental Protection Agency. Environmental Sampling and Analytical Methods (ESAM) Program. Method 6010D (SW-846): inductively coupled plasma atomic emission spectrometry, revision 4. Washington, DC (2014). Available at: <https://www.epa.gov/esam/epa-method-6010d-sw-846-inductively-coupled-plasma-atomic-emission-spectrometry> (Accessed: 19 September 2022).
- [23] Naso F, Gandaglia A, Bottio T, Tarzia V, Nottle MB, d'Apice AJF, *et al.* First quantification of alpha-Gal epitope in current glutaraldehyde-fixed heart valve bioprostheses. *Xenotransplantation*. 2013; 20: 252–261.
- [24] Lim HG, Choi SY, Yoon EJ, Kim SH, Kim YJ. In vivo efficacy of alpha-galactosidase as possible promise for prolonged durability of bioprosthetic heart valve using alpha1,3-galactosyltransferase knockout mouse. *Tissue Engineering. Part a*. 2013; 19: 2339–2348.
- [25] Schoen FJ, Levy RJ. Calcification of tissue heart valve substitutes: progress toward understanding and prevention. *The Annals of Thoracic Surgery*. 2005; 79: 1072–1080.
- [26] Agathos EA, Tomos PI, Kostomitsopoulos N, Koutsoukos PG. A novel anticalcification treatment strategy for bioprosthetic valves and review of the literature. *Journal of Cardiac Surgery*. 2019; 34: 895–900.
- [27] Zilla P, Weissenstein C, Bracher M, Human P. The anticalcific effect of glutaraldehyde detoxification on bioprosthetic aortic wall tissue in the sheep model. *Journal of Cardiac Surgery*. 2001; 16: 467–472.
- [28] Galli C. Animal engineering for xenotransplantation. *European Journal of Transplantation*. 2023; 1: 182–191.
- [29] Simon P, Kasimir MT, Seebacher G, Weigel G, Ullrich R, Salzer-Muhar U, *et al.* Early failure of the tissue engineered porcine heart valve SYNERGRAFT in pediatric patients. *European Journal of Cardio-thoracic Surgery: Official Journal of the European Association for Cardio-thoracic Surgery*. 2003; 23: 1002–1006; discussion 1006.
- [30] Calafiore AM, Haverich A, Gaudino M, Di Mauro M, Fattouch K, Prapas S, *et al.* Immunoreaction to xenogenic tissue in cardiac surgery: alpha-Gal and beyond. *European Journal of Cardio-thoracic Surgery: Official Journal of the European Association for Cardio-thoracic Surgery*. 2022; 62: eza115.
- [31] Mangold A, Szerafin T, Hoetzenecker K, Hacker S, Lichtenauer M, Niederpold T, *et al.* Alpha-Gal specific IgG immune response after implantation of bioprostheses. *The Thoracic and Cardiovascular Surgeon*. 2009; 57: 191–195.
- [32] Böer U, Buettner FFR, Schridde A, Klingenberg M, Sarikouch S, Haverich A, *et al.* Antibody formation towards porcine tissue in patients implanted with crosslinked heart valves is directed to antigenic tissue proteins and α Gal epitopes and is reduced in healthy vegetarian subjects. *Xenotransplantation*. 2017; 24: 10.1111/xen.12288.
- [33] Konakci KZ, Bohle B, Blumer R, Hoetzenecker W, Roth G, Moser B, *et al.* Alpha-Gal on bioprostheses: xenograft immune response in cardiac surgery. *European Journal of Clinical Investigation*. 2005; 35: 17–23.
- [34] Galili U. Biosynthesis of α -Gal Epitopes (Gal α 1-3Gal β 1-4GlcNAc-R) and Their Unique Potential in Future α -Gal Therapies. *Frontiers in Molecular Biosciences*. 2021; 8: 746883.
- [35] Milland J, Christiansen D, Lazarus BD, Taylor SG, Xing PX, Sandrin MS. The molecular basis for galal-pha(1,3)gal expression in animals with a deletion of the alpha1,3galactosyltransferase gene. *Journal of Immunology (Baltimore, Md.: 1950)*. 2006; 176: 2448–2454.
- [36] Boutin M, Sun Y, Shacka JJ, Auray-Blais C. Tandem Mass Spectrometry Multiplex Analysis of Glucosylceramide and Galactosylceramide Isoforms in Brain Tissues at Different Stages of Parkinson Disease. *Analytical Chemistry*. 2016; 88: 1856–1863.
- [37] Yu RK, Nakatani Y, Yanagisawa M. The role of glycosphingolipid metabolism in the developing brain. *Journal of Lipid Research*. 2009; 50: S440–S445.
- [38] Feingold KR. Thematic review series: skin lipids. The role of epidermal lipids in cutaneous permeability barrier homeostasis. *Journal of Lipid Research*. 2007; 48: 2531–2546.
- [39] Muralidharan S, Shimobayashi M, Ji S, Burla B, Hall MN, Wenk MR, *et al.* A reference map of sphingolipids in murine tissues. *Cell Reports*. 2021; 35: 109250.
- [40] Shao A, Xu L, Wu X, Liu S, Lu Y, Fan C. Gal epitope expression and immunological properties in iGb3S deficient mice. *Sci-*

- entific Reports. 2018; 8: 15433.
- [41] Murray-Segal L, Gock H, Cowan PJ, d'Apice AJF. Anti-Gal antibody-mediated skin graft rejection requires a threshold level of Gal expression. *Xenotransplantation*. 2008; 15: 20–26.
 - [42] Butler JR, Skill NJ, Priestman DL, Platt FM, Li P, Estrada JL, *et al.* Silencing the porcine iGb3s gene does not affect Gal α 3Gal levels or measures of anticipated pig-to-human and pig-to-primate acute rejection. *Xenotransplantation*. 2016; 23: 106–116.
 - [43] Angiolillo A, Gandaglia A, Arcaro A, Carpi A, Gentile F, Naso F, *et al.* Altered Blood Levels of Anti-Gal Antibodies in Alzheimer's Disease: A New Clue to Pathogenesis? *Life* (Basel, Switzerland). 2021; 11: 538.
 - [44] Dahl K, Buschard K, Gram DX, d'Apice AJF, Hansen AK. Glucose intolerance in a xenotransplantation model: studies in alpha-gal knockout mice. *APMIS: Acta Pathologica, Microbiologica, et Immunologica Scandinavica*. 2006; 114: 805–811.
 - [45] Sørensen DB, Dahl K, Ersbøll AK, Kirkeby S, d'Apice AJF, Hansen AK. Aggression in cataract-bearing alpha-1,3-galactosyltransferase knockout mice. *Laboratory Animals*. 2008; 42: 34–44.
 - [46] Tearle RG, Tange MJ, Zannettino ZL, Katerelos M, Shinkel TA, Van Denderen BJ, *et al.* The alpha-1,3-galactosyltransferase knockout mouse. Implications for xenotransplantation. *Transplantation*. 1996; 61: 13–19.
 - [47] Samadi A, Buro J, Dong X, Weinstein A, Lara DO, Celie KB, *et al.* Topical α -Gal Nanoparticles Enhance Wound Healing in Radiated Skin. *Skin Pharmacology and Physiology*. 2022; 35: 31–40.
 - [48] Perota A, Lagutina I, Duchi R, Zanfrini E, Lazzari G, Judor JP, *et al.* Generation of cattle knockout for galactose- α 1,3-galactose and N-glycolylneuraminic acid antigens. *Xenotransplantation*. 2019; 26: e12524.
 - [49] U.S. Food and Drug Administration. 2020. Available at: <https://www.fda.gov/news-events/press-announcements/fda-approves-first-its-kind-intentional-genomic-alteration-line-domestic-pigs-both-human-food#:~:text=This%20is%20the%20first%20IGA,surface%20of%20the%20pigs'%20cells> (Accessed: 11 January 2024).
 - [50] Perota A, Galli C. N-Glycolylneuraminic Acid (Neu5Gc) Null Large Animals by Targeting the CMP-Neu5Gc Hydroxylase (CMAH). *Frontiers in Immunology*. 2019; 10: 2396.
 - [51] Soulillou JP, Padler-Karavani V. Editorial: Human Antibodies Against the Dietary Non-human Neu5Gc-Carrying Glycans in Normal and Pathologic States. *Frontiers in Immunology*. 2020; 11: 1589.
 - [52] Reardon S. First pig-to-human heart transplant: what can scientists learn? *Nature*. 2022; 601: 305–306.
 - [53] Moazami N, Stern JM, Khalil K, Kim JI, Narula N, Mangiola M, *et al.* Pig-to-human heart xenotransplantation in two recently deceased human recipients. *Nature Medicine*. 2023; 29: 1989–1997.
 - [54] Cramer M, Chang J, Li H, Serrero A, El-Kurdi M, Cox M, *et al.* Tissue response, macrophage phenotype, and intrinsic calcification induced by cardiovascular biomaterials: Can clinical regenerative potential be predicted in a rat subcutaneous implant model? *Journal of Biomedical Materials Research. Part a*. 2022; 110: 245–256.